

Study of TiO₂ Deactivation during Gaseous Acetone Photocatalytic Oxidation

A. V. Vorontsov,^{*,1} E. N. Kurkin,[†] and E. N. Savinov^{*}

^{*}Boreskov Institute of Catalysis, pr.Ak. Lavrentieva, 5, Novosibirsk, 630090, Russian Federation; and [†]Institute on New Chemical Problems, Chernogolovka, Moskow Region 142432, Russian Federation

Received January 22, 1999; revised April 12, 1999; accepted May 20, 1999

The kinetics of the deep photocatalytic oxidation of acetone was studied. Special attention was paid to the thermal deactivation process. The rate of the reaction reaches a peak at about 100°C. With increasing concentration of water vapor the peak shifts towards higher temperature, whereas with increasing acetone concentration the peak shifts towards lower temperature. An increase in water vapor concentration slightly decreases the rate of oxidation at 40°C and increases it at temperatures above the rate maximum. The presence of two types of acetone adsorption sites was deduced from two $\nu_{C=O}$ bands of adsorbed acetone at 1683 and 1710 cm⁻¹ and can explain the dependence of the rate on acetone concentration. The rate of oxidation increases at temperatures below the peak, mainly because of the increase in the rate coefficient at the sites of the first type. This behavior has been ascribed to the thermal oxidation of an intermediate of the photocatalytic process. Abrupt drop in rate at temperatures above the peak is due to the partial oxidation products of acetone thermal oxidation that modify the TiO₂ surface. © 1999

Academic Press

Key Words: acetone photocatalytic oxidation; deactivation; kinetics.

INTRODUCTION

Over the past decade there has been growing interest in photocatalytic oxidation as a means of pollution destruction. This interest has been purely academic for more than half a century. Today, photocatalytic oxidation is recognized as a method for purifying air and water. Thus, most studies of photocatalytic processes are now carried out in reactors that may be prototypes of commercial purification systems. The main features of many photocatalytic oxidation reactions have been studied in such systems. These reactors, however, do not allow the detection of precise microkinetic characteristics of the reaction itself because of varying concentrations of reactants and uneven light distribution throughout the photocatalyst. In addition, the re-

actors cannot be scaled up easily to commercial systems. The creation of such systems demands macrokinetic calculations of performance based on microkinetic data and reaction mechanisms. This paper will present kinetic data of the acetone photocatalytic oxidation on TiO₂ at steady state and uniform distribution of concentrations.

Photocatalytic oxidation of acetone in the gas phase has been discussed in several recent publications (1–5). Acetone is oxidized on the surface of TiO₂ more rapidly than other organic compounds such as toluene and chloroform. No gaseous intermediates of oxidation were detected. It was reported that the rate of oxidation follows the Langmuir–Hinshelwood equation. Influence of water vapor on the reaction rate was satisfactorily described by competitive adsorption according to Langmuir isotherm. The temperature dependence of the rate of complete photocatalytic oxidation of acetone was first studied in (5). Oxidation is quicker as temperature increases to 80°C, and with a further increase in temperature it begins to slow down. The rate at 163°C is about five times lower than at 80°C. This rather quick decrease in activity upon heating was explained by catalyst deactivation: the catalyst turned brown after reaction at a high temperature, and gradually regained activity during the run at 72°C. However, the nature of this deactivation remained unclear.

A similar temperature dependence of the photocatalytic oxidation rate of organics was described by Lyashenko *et al.* (6). They studied the oxidation of propene and butene in a flow-circulation reactor and detected a maximum reaction rate at 90 to 110°C. The reaction rate was very low over the temperature range 150 to 240°C; above 240°C the rate increased, and a thermal oxidation reaction occurred. These authors assumed that the low rate of photocatalytic oxidation at high temperature was related to temperature changes in the photocatalyst surface, namely, a depletion of active oxygen species.

Falconer *et al.* observed temperature deactivation of TiO₂ for acetaldehyde oxidation (7). The reaction rate was already at 90°C quite low but it gradually reaches its initial value after running the reaction at room temperature.

¹Correspondence author. Temporary address for 1999: Chemical Engineering Department, 697 Rhodes Hall, University of Cincinnati, Cincinnati, OH 45221-0171. E-mail: avoronts@alpha.che.uc.edu.

However, not all photocatalytic oxidation reactions in the gas phase exhibit thermal deactivation. Photocatalytic oxidation of CO does not show a temperature maximum, and the reaction rate increases in the temperature range studied, 40 to 230°C (8, 9).

This paper describes the kinetics of acetone oxidation as related to catalyst thermal deactivation. Because thermal deactivation during photocatalytic oxidation of very different organics begins in close temperature intervals, it seems plausible that the mechanisms of deactivation have much in common and there is some discretion in choosing substrate. To study the deactivation process we have chosen acetone as model compound for (a) during acetone oxidation no intermediate gaseous products are formed, which simplifies analysis of kinetics, and (b) acetone is not as easily oxidized as acetaldehyde and is not readily involved in condensation reactions. Kinetic measurements were performed in a flow-circulation reactor because this reactor ensures uniform distribution of reactant concentrations throughout the system.

EXPERIMENTAL

Titanium dioxide was prepared by aqueous hydrolysis of chemically pure TiCl₄ and precipitated with NaOH. The deposit formed was washed thoroughly with distilled water, dried, and calcined in air for 3 h at 400°C. TEM investigation revealed that the primary titania particles are of high crystallinity with a typical primary particles size of 8 to 13 nm, and they form larger aggregates of 300 to 800 nm. The specific surface area of this photocatalyst was 120 m²/g, as determined by the BET method. X-ray analysis revealed the presence of anatase only.

UV-VIS diffuse reflectance spectra were recorded using a Shimadzu UV-300 spectrophotometer. MgO was a reference specimen, and its reflectance was assumed to be 85% throughout the spectrum.

Kinetic measurements were performed in a flow-circulation system described elsewhere (5). This system includes a quartz reactor with an optical quartz window, a membrane circulation pump, and stainless steel connection pipes. The reactor was placed in a temperature-controlled box to keep the temperature in the range 40 to 140°C. The circulation rate, determined by the pump, was about 5 liter/min, 100 times higher than the maximum input flow rate used. Therefore, the reactor can be considered to be a perfect stirred reactor without concentration and temperature gradients.

Oxygen in air was used as the oxidant. The input gas flow was prepared according to the following procedure. Purified air from an air line was divided into three flows, one of which was passed through a saturator filled with water to attain the necessary water vapor concentration. The second flow was passed through a saturator with acetone, and the third flow was used to dilute the gas mixture after the convergence

of all the flows. Dilution is essential because the acetone equilibrium vapor pressure is rather high.

Input and output gas mixtures were analyzed using gas chromatographs equipped with FID and TCD detection. Carbon dioxide was determined by analyzing methane with FID after methanation of a gas probe.

For kinetic measurements, TiO₂ was applied to glass plates from an aqueous slurry. The area of the specimen spot was 3 cm².

Specimens in the quartz reactor were irradiated by a 1000 W xenon lamp, the light of which was transmitted through a 313-nm interference filter. The incident light intensity was 7 mW/cm².

The rate of acetone oxidation was calculated from the rate of evolution of the deep oxidation product, CO₂. Measurements of the CO₂ concentration were performed until steady state was reached, and only steady state measurements were used to calculate the oxidation rate. Typically, steady state was attained in 30 min below 80°C but took longer to reach at higher temperatures. The maximum estimated error in the reaction rate data is 10%.

RESULTS

Water vapor is known to significantly influence the photocatalytic oxidation rates and reaction paths. We checked this influence on our photocatalyst at low, almost ambient temperature. An increase (by 29) in the water vapor concentration 700 to 20400 ppm led to a decrease by only about 1.5 in the acetone oxidation rate (Fig. 1). This dependence

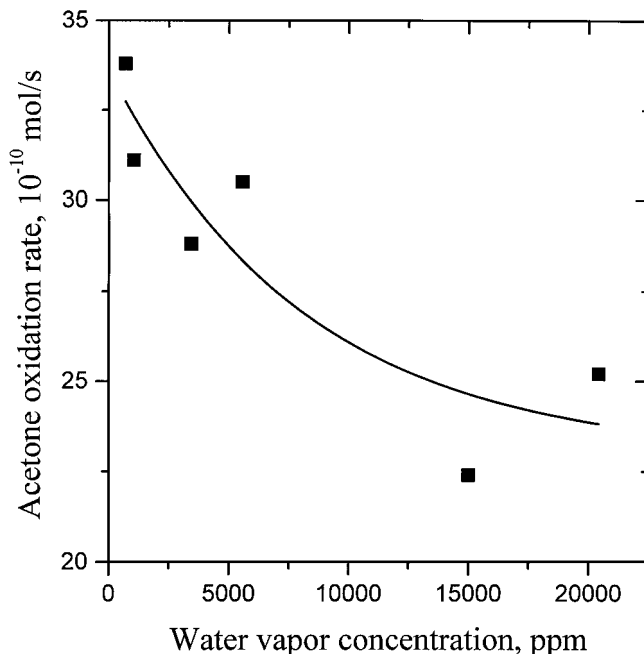


FIG. 1. Effect of water vapor on the photocatalytic oxidation rate of acetone. Temperature 40°C, acetone concentration 500 ppm.

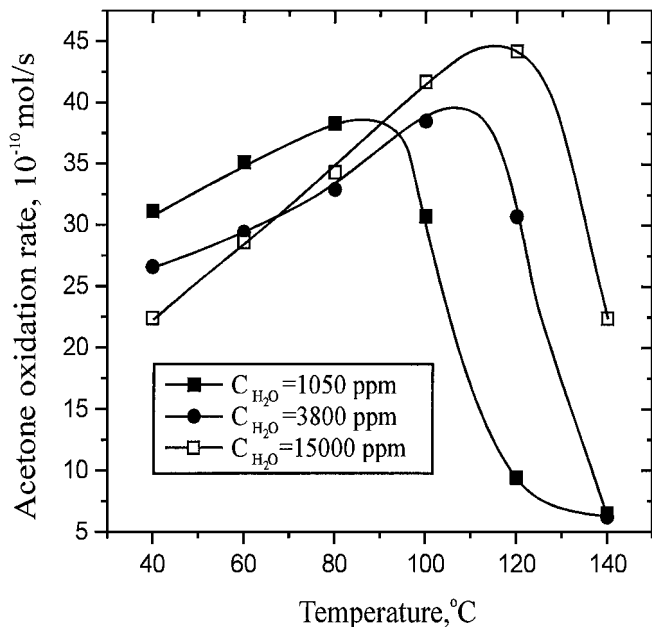


FIG. 2. Influence of water vapor concentration on temperature dependence of photocatalytic oxidation of acetone. Acetone concentration 500 ppm.

was determined by measuring the reaction rate at random water vapor concentrations. Thus, the broad scatter in Fig. 2 may be due to the abrupt switch from the ascending part of the water adsorption isotherm to the descending part, the difference being due to incomplete equilibrium. This scatter does not exceed the error of the reaction rate measurements, however. The curve in Fig. 1 represents an average response of the photocatalyst to changes in the water vapor concentration.

Figure 2 demonstrates how the water vapor concentration affects the temperature dependence of the oxidation rate between 40 and 140°C. Just as in our earlier work on a different TiO₂ (5), a maximum in the temperature dependence is observed at about 100°C. At low water vapor concentration, the reaction rate decreases already above 80°C, while at higher water vapor concentrations, the reaction rate reaches its maximum at a higher temperature, e.g., at 120°C for 15000 ppm. In the high temperature region, the dependence of the rate on water vapor concentration changes; an increase in water vapor concentration results in an increase in the reaction rate. Moreover, high water vapor concentration (15000 ppm) enhances the peak reaction rate. Thus, water vapor inhibits the temperature deactivation of the photocatalyst.

The next two figures pertain to the influence of the acetone concentration on the reaction rate. Figure 3 shows the concentration dependence of the reaction rate at 40 and 80°C. Each was recorded using fresh catalyst and increasing the acetone concentration at constant temperature and constant water vapor concentration. Higher tem-

peratures were not used since temperature deactivation would obscure the concentration dependence. The reaction rate is significantly higher at 80°C than at 40°C over the whole range of concentrations studied (25–3000 ppm). The Langmuir–Hinshelwood equation is often used to describe such dependence in photocatalysis. Since the water vapor concentration is nearly constant for all the results in Fig. 3, the Langmuir–Hinshelwood equation that takes into account the adsorption of water (*w*) as well as acetone (*a*),

$$W = \frac{kK_aC_a}{1 + K_aC_a + K_wC_w},$$

can be reduced to a form that does not contain parameters for water adsorption,

$$W = \frac{kKCa}{1 + KCa}, \quad [1]$$

by substitution of *K* for *K_a/(1 + K_wC_w)*. The dashed lines in Fig. 3 represent the fits of the experimental points by Eq. [1]. It is clear that the Langmuir–Hinshelwood equation applied to one type of adsorption site describes both concentration dependencies unsatisfactorily. These dependencies are, however, excellently fitted by a Langmuir–Hinshelwood equation with two different surface adsorption sites (solid lines in Fig. 3):

$$W = \frac{k_1K_1C_a}{1 + K_1C_a} + \frac{k_2K_2C_a}{1 + K_2C_a}. \quad [2]$$

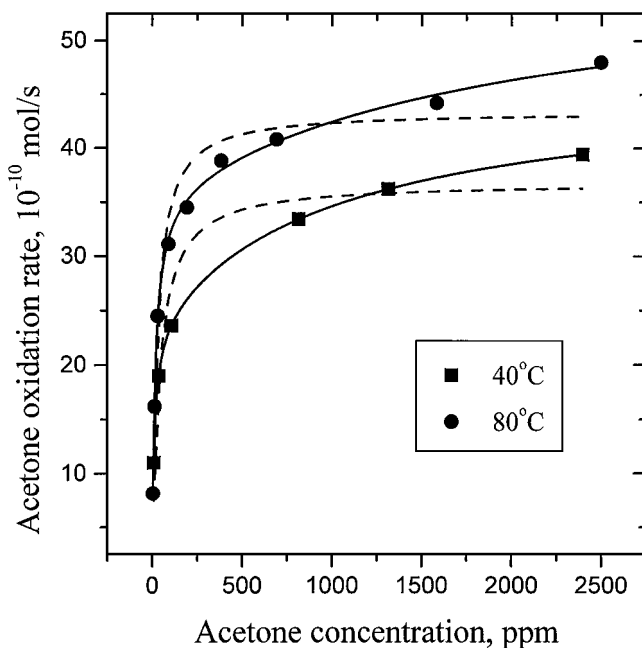


FIG. 3. Dependence of the acetone photocatalytic oxidation rate on acetone concentration at 40 and 80°C. Water vapor concentration 4500 ppm. Dashed and solid lines represent the single- and double-site Langmuir–Hinshelwood models, respectively.

TABLE 1
Parameters of Langmuir–Hinshelwood Eq. [2] for Curves in Fig. 3

Temperature (°C)	k_1 (10^{-10} mol/s)	K_1 (ppm ⁻¹)	k_2 (10^{-10} mol/s)	K_2 (ppm ⁻¹)
40	23.8 ± 0.4	0.088 ± 0.0007	22.5 ± 0.8	0.00097 ± 0.00002
80	36.2 ± 5.9	0.062 ± 0.006	22.1 ± 9.9	0.00044 ± 0.00032

The adsorption constants K_1 and K_2 in this equation incorporate the influence of water vapor just as in Eq. [1]. The parameters of Eq. [2] for the curves in Fig. 3 are given in Table 1. The two sites differ significantly in adsorption constants, one constant being about two orders of magnitude larger than the other one. An increase in temperature causes an increase in the rate coefficient for the first type of sites, k_1 , whereas no substantial change is observed for the second type of sites. The adsorption constants for both types of sites decrease with increasing temperature. The main temperature change in the parameters of Eq. [2] is concentrated in k_1 that is 1.5 times larger at 80°C than at 40°C. The presence of two types of adsorption sites is corroborated by FTIR spectrum of TiO₂ operated in acetone oxidation at 40°C. There are two bands for $\nu_{C=O}$ at 1683 and 1710 cm⁻¹.

The influence of the acetone concentration on the reaction rate was investigated at higher temperatures by exchange of parameters varied quicker and slower. In contrast to the measurements described above, a freshly prepared catalyst was held at constant concentrations of acetone and

water vapor, while the temperature increased. The dependencies obtained are given in Fig. 4. It is seen that an increase in acetone concentration results in a shift in the maximum reaction rate temperature to lower values. Like the dependence on water vapor concentration, the dependence on acetone concentration changes in the high temperature range. Above 115°C, the highest concentration has the lowest reaction rate. The peak reaction rates were close for acetone concentrations of 50 and 2000 ppm, but this reaction rate is somewhat lower for an acetone concentration of 500 ppm. The rate of decrease in activity at temperatures above the maximum increases with increasing acetone concentration. No CO₂ formation was detected in the dark at any temperature.

At temperatures below the maximum rate, steady state conditions in the reactor are established within 30 min. The main time-limiting process is adsorption on the photocatalyst, as proved by the fact that smaller amounts of photocatalyst led to shorter relaxation times. The situation changes at higher temperatures. The time taken to reach steady state conditions increases to 100 min. Figure 5 shows

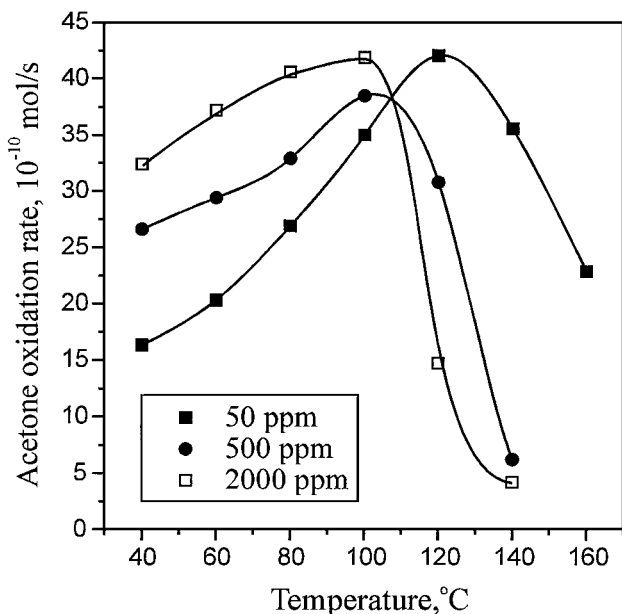


FIG. 4. Influence of acetone concentration on temperature dependence of the photocatalytic oxidation rate of acetone. Acetone concentrations for respective curves are given in the frame. Water vapor concentration 5000 ppm.

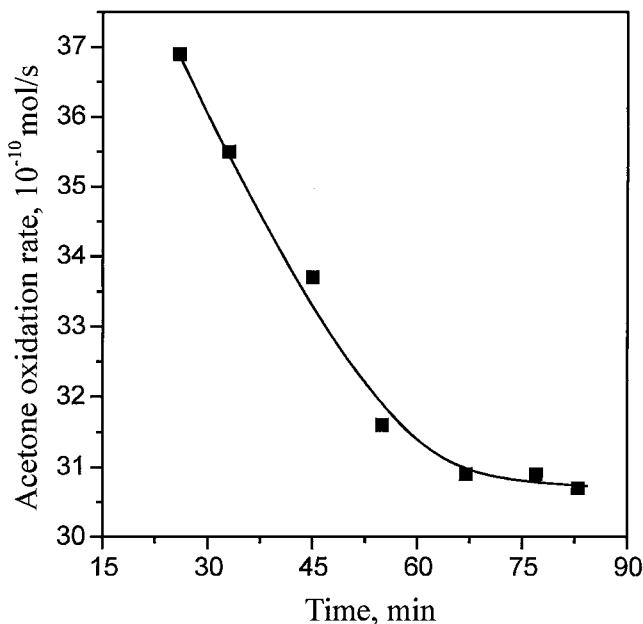


FIG. 5. Decay of photocatalytic oxidation rate of acetone after increase in temperature from 100°C to 120°C. Water vapor concentration 4000 ppm, acetone concentration 500 ppm.

a time profile of the reaction rate after an increase in temperature from 100 to 120°C. The reaction rate decreased gradually for 60 min until it became steady.

The temperature deactivation described above can be attributed either to temperature changes in the photocatalyst surface itself, e.g., depletion of active oxidizing oxygen species (Lyashenko *et al.* (6) and Formenti *et al.* (10)), or to changes in the photocatalyst due to participation in the reaction at a high temperature. To distinguish between these alternatives, a fresh sample of photocatalyst was kept in the reactor for 1.5 h at 140°C under the conditions of thermal deactivation but without acetone vapor. The flow of acetone vapor was then switched on and the concentration of acetone in the reactor began to increase. If the catalyst deactivates when it is heated, then it should deactivate after being kept for 1.5 h at 140°C. Figure 6 shows that, after adding acetone, the activity was initially rather high but was quickly followed by the start of deactivation, a low steady state rate was established in 30 min.

At temperatures below 80°C, the rates of acetone consumption and CO₂ formation are in good stoichiometric accordance at a steady state rate of CO₂ formation; that is, the rate of CO₂ evolution is three times higher than the rate of acetone consumption. However, at higher temperatures there is a considerable difference between these stoichiometric rates. For instance, at 140°C, and an acetone concentration of 550 ppm and a water concentration of 4000 ppm, the rate of acetone consumption after 100 min of opera-

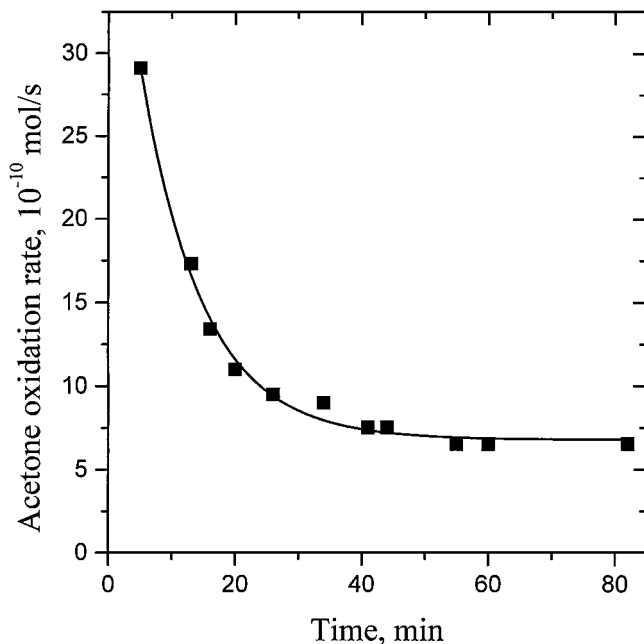


FIG. 6. Decrease in photocatalytic oxidation rate of acetone at 140°C after the addition of acetone to the reactor. Water vapor concentration 5000 ppm, steady state concentration of acetone 500 ppm. Before the addition of acetone TiO₂ was operated at 140°C for 1.5 h.

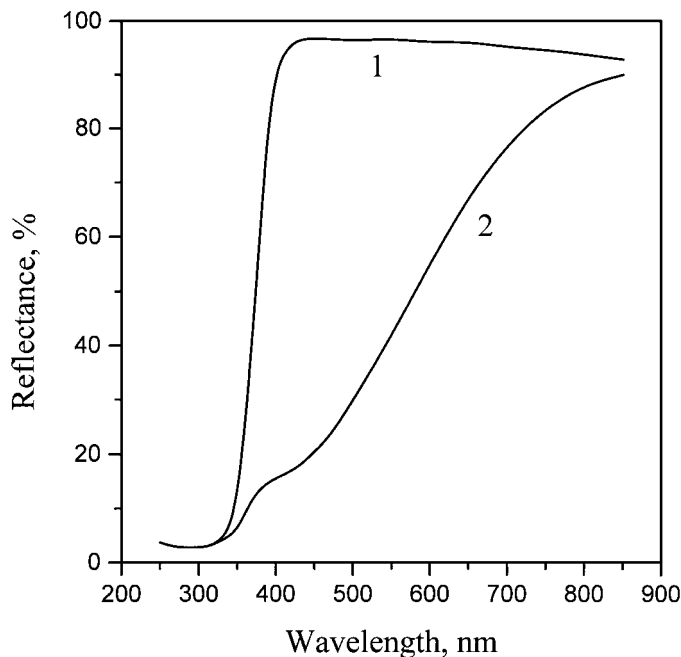


FIG. 7. UV-VIS diffuse reflectance spectra of (1) initial TiO₂ and (2) TiO₂ after run with deactivation at 140°C for 1 h.

tion is almost equal to the rate of CO₂ evolution. The catalyst changes color from white to brown during operation at temperatures above the peak rate. UV-VIS spectra of the initial catalyst and the brown deactivated catalyst are shown in Fig. 7. Since we used glass plates for catalyst deposition it was possible to control the color of the catalyst at its backside. Although the thickness of the catalyst film was sufficient to absorb all incident light, the backside also turned brown. This change in color can, thus, be attributed to a thermal reaction, as corroborated by the following experiment. Freshly deposited TiO₂ was kept in the reactor in the dark at 140°C, with 500 ppm of acetone and 4500 ppm of H₂O, for 1.5 h. The catalyst turned brown. After the light was turned on, the rate of acetone oxidation was steady and low and equal to the steady rate in Fig. 6.

The difference between the rate of acetone consumption and the rate of CO₂ formation at deactivation temperatures is probably due to a low rate of acetone diffusion into the deeper layers of the catalyst where acetone is consumed in a thermal reaction resulting in the accumulation of surface products.

DISCUSSION

Considering the TEM images of the photocatalyst leads us to conclude that most of the primary particles in this material are stuck together in large aggregates. The framework of primary particles has pore diameter close to the radius of the particles. Even if a fraction of the pores have a

diameter of 2 nm, according to the Kelvin equation, capillary condensation of water will take place at relative water pressures above 0.3. The highest concentration of water was 20000 ppm at 40°C, which corresponds to a relative water vapor pressure of 0.27 (11). The highest relative pressure of acetone was much lower than this. This strongly suggests that capillary condensation plays no role in the above results.

The acetone coverage of the photocatalyst surface at 40°C, under 2500 ppm of acetone and 4500 ppm of water, as calculated from data in Table 1, is 0.99 and 0.7 for adsorption sites of the first and second types, respectively. Water molecules are more polar than those of acetone. Therefore a higher water coverage is to be expected under the same conditions. The high boiling point of water makes it possible for water to form multilayers in experiments employing high water concentrations. This multilayer water coverage may represent significant difficulty for the transport of oxygen to the surface of the photocatalyst, since the solubility of oxygen in water is rather low. The solubility of acetone in water is infinite, and water multilayers will not influence the acetone concentration at the surface of the photocatalyst. At a relative pressure below 0.5, according to the BET equation the surface coverage increases very slowly with increasing relative pressure and does not exceed 2. Thus, the weak influence of water vapor on the reaction rate can be attributed to the formation of monolayer water coverage at a low water vapor pressure.

The difference between the amounts of acetone consumed and CO₂ formed at temperatures of deactivation clearly testifies to the accumulation of surface products. Figure 6 demonstrates that it is the presence of acetone at a high temperature that causes deactivation. Therefore, this decrease in activity can be assigned to a negative influence of the accumulated surface products. These surface products result from thermal oxidation of acetone: a non-illuminated photocatalyst turned brown after deactivation just as an illuminated one. Accumulation of partial thermal oxidation products also caused thermal deactivation of TiO₂ during acetaldehyde oxidation (7). At the temperatures of deactivation, water cannot form multilayers on the photocatalyst surface because of the very low relative water vapor pressure, but water will compete with acetone for adsorption sites. Both the increase in the concentration of water vapor and the decrease in the concentration of acetone vapor reduce the acetone coverage and the rate at which surface products of acetone oxidation are formed; therefore, the peak in the oxidation rate curve shifts to higher temperatures (Figs. 2 and 4). Sitkiewitz and Heller (12) observed similar influence of water vapor on TiO₂ deactivation during photocatalytic oxidation of gaseous benzene. With water in feed stream, the rate of oxidation was consistent for 300 h, while deactivation developed quickly in the absence of water.

According to Fig. 3, we assume that there are two types of adsorption sites on the surface of the photocatalyst employed for acetone oxidation. The difference of two orders of magnitude between adsorption constants on these sites implies that they are very different types. The presence of two bands for $\nu_{C=O}$ in the FTIR spectrum at 1683 and 1710 cm⁻¹ allows us to assign the first type to coordinately unsaturated surface Ti⁴⁺ ions and the second type of sites to surface OH groups. These two types of sites were also suggested by Nimlos *et al.* for ethanol adsorption during photocatalytic oxidation (13).

The next question is: why does the rate of deep photocatalytic oxidation of acetone increase with temperature before it reaches a maximum? It follows from Table 1 that the major increase in reaction rate results from an increase in the rate coefficient for the first type of sites. As shown earlier in studies on the correlation of photocatalytic activity with the activity in oxygen isotopic exchange (14–16), the rate of photocatalytic oxidation is limited by the rate of production of active oxygen oxidizing species. Active oxygen species are formed by the capture of photogenerated charge carriers by molecular oxygen and surface lattice oxygen as well as by water and hydroxyl groups. The rate of these reactions can hardly be temperature dependent and is most probably determined by the availability of holes and electrons. The rate coefficient k_1 in Eq. [2] is an integral characteristic of the deep oxidation reaction on the first type of sites. It includes the rate characteristic of thermal partial oxidation reactions. Thus, the increase in k_1 with temperature is probably due to thermal oxidation reactions which lead from an intermediate of acetone oxidation to other more deeply oxidized intermediates. The first intermediate is most probably formaldehyde, which is oxidized thermally to formic acid or surface carbonates. Indeed, we detected traces of formaldehyde during acetone oxidation at elevated temperature. Some yellow coloration was observed in nonilluminated parts of the photocatalyst, even at a temperature below the maximum rate. This coloration is attributed to products of thermal oxidation reaction of formaldehyde.

CONCLUSION

The rate of the deep photocatalytic oxidation of acetone peaks at a temperature of about 100°C. An increase in the water vapor concentration at 40°C slightly decreases the rate of oxidation. At a temperature above the rate peak, the increase in the water vapor concentration results in the increase in the rate of oxidation. This increase shifts the rate peak to higher temperature.

The rate peak shifts to lower temperatures with increasing acetone concentration. The dependence of the rate on acetone concentration as well as the FTIR spectrum of

adsorbed acetone suggest that there are two types of adsorption sites of acetone on the TiO₂ surface.

The increase in the oxidation rate with temperature below the peak is due to a thermal oxidation reaction of intermediates of the photocatalytic process leading to other, more oxidized intermediates. The drop in photocatalytic activity at temperatures above the peak results from an accumulation of acetone partial oxidation products produced by a thermal reaction.

Further studies will focus on what happens to this photocatalyst during deactivation. Surface intermediates will be detected and a mechanism for the whole process will be proposed.

ACKNOWLEDGMENT

The Russian Federal Program "Integration" supported this work.

REFERENCES

1. Peral, J., and Ollis, D. F., *J. Catal.* **136**, 554 (1992).
2. Sauer, M. L., and Ollis, D. F., *J. Catal.* **149**, 81 (1994).
3. Alberici, R. M., and Jardim, W. F., *Appl. Catal. B Environ.* **14**, 55 (1997).
4. Muradov, N. Z., T-Raissi, A., Muzzey, D., Painter, C. R., and Kemme, M. R., *Solar Energy* **56**, 445 (1996).
5. Vorontsov, A. V., Savinov, E. N., Barannik, G. B., Troitsky, V. N., and Parmon, V. N., *Catal. Today* **39**, 207 (1997).
6. Lyashenko, L. V., Gorokhovatsky, Ya. B., Stepanenko, V. I., and Yampolskaya, F. A., *Theor. Exp. Chem.* **13**, 35 (1977). [In Russian]
7. Falconer, J. L., and Magrini-Bair, K. A., *J. Catal.* **179**, 171 (1998).
8. Vorontsov, A. V., Savinov, E. N., Kurkin, E. N., Torbova, O. D., and Parmon, V. N., *React. Kinet. Catal. Lett.* **62**, 83 (1997).
9. Lyashenko, L. V., and Gorokhovatsky, Ya. B., *Theor. Exp. Chem.* **10**, 186 (1974). [In Russian]
10. Formenti, M., Juillet, F., Meriaudeau, P., and Teichner, S. J., *Chem. Techn.* **1**, 680 (1971).
11. Weasts, R. C., Ed., "Handbook of Chemistry and Physics," 56th ed. CRC Press, Boca Raton, FL, 1975.
12. Sitkiewitz, S., and Heller, A., *New J. Chem.* **20**, 233 (1996).
13. Nimlos, M. R., Wolfrum, E. J., Brewer, M. L., Fennel, J. A., and Bintner, G., *Environ. Sci. Technol.* **30**, 3102 (1996).
14. Courbon, H., Formenti, M., and Pichat, P., *J. Phys. Chem.* **81**, 550 (1977).
15. Sato, S., Kadowaki, T., and Yamaguti, K., *J. Phys. Chem.* **88**, 2930 (1984).
16. Sato, S., and Kadowaki, T., *J. Catal.* **106**, 295 (1987).